Composites Part B 220 (2021) 108983

Contents lists available at ScienceDirect

Composites Part B

journal homepage: www.elsevier.com/locate/compositesb

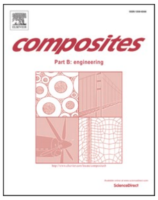

π - π interaction between carbon fibre and epoxy resin for interface improvement in composites

Lei Zeng [a], Xuqing Liu [a,b,*], Xiaogang Chen [a,b], Constantinos Soutis [a,b]

[a] Department of Materials, School of Natural Sciences, University of Manchester, Manchester, M13 9PL, United Kingdom
[b] Aerospace Research Institute, University of Manchester, Manchester, M13 9PL, United Kingdom

ARTICLE INFO

Keywords:
Interface
π-bonding
Polydopamine
Graphene oxide
Polymer-matrix composites (PMCs)

ABSTRACT

This paper reports on a new biomimetic method for modifying carbon fibre surface aiming to improve the bonding between the fibre and an epoxy resin system. Inspired by the composition of adhesive proteins in mussels, dopamine was utilised in the process that was allowed to be self-polymerised onto the carbon fibre surface via π-π interaction to form a nano-thin surface-adherent polydopamine (PDA) layer. Graphene oxide (GO) was also grafted on the carbon fibre to increase interfacial strength of the composites. The fibre surface treatment and modification were performed at ambient temperature, which is non-damaging to the fibre. The chemical deposition and functional groups on the fibre were characterised by X-ray Photoelectron Spectroscopy, while the chemical structure of solution and fibre were investigated by Raman Spectroscopy. Micro-bond tests showed that the fibre/resin interfacial shear strength (IFSS) was increased by almost 70%, while the tensile strength of the GO-PDA carbon fibre improved by approximately 80%. The research indicated that π-π interaction-based fibre modification has the potential of improving crack resistance of fibre reinforced polymer composites, preventing or delaying matrix cracking and delamination that can affect their fatigue performance.

1. Introduction

Carbon fibre reinforced plastics (CFRP) have been widely used in aerospace, automobile, defence industries and high quality consumer products due to their high specific strength, modulus, lightweight and flexible design [1]. The composite performance depends on the properties of its constituents and on the properties of the interface between the polymer matrix and reinforcing fibres [2]. Two main damage mechanisms have been identified in multi-layered composite plates; one occurs within the lamina (intra-laminar), in the form of resin cracking and fibre breakage, while the other mode is ply separation or delamination, termed as inter-laminar cracking [3]. Much effort has been invested into optimisation of composite interfacial properties. In the case of carbon fibre composites that are widely used for different structural applications, the surface of the carbon fibre is chemically inert, and the manufactured reinforced polymer composite does not always achieve expectations derived from the properties of its constituents [4–7]. Hence, it is of particular importance to achieve good bonding between fibre and matrix. Fibre surface modification has been critical to improve composite interfacial properties and ultimately structural performance.

In general, the fibre surface modification process concentrated on achieving high specific area, good chemical activity and superior mechanical properties. As a new development, 2D materials such as graphene oxide (GO) have attracted interest since it offers a high specific area with flexibility in addition to attractive mechanical properties, thermal and electrical conductivity [8–11]. Graphene oxide is chemically more active with the fibre and epoxy resin than graphene due to the epoxide and hydroxyl groups within the GO sheets and carbonyl and carboxyl at the edges of these sheets [12–14]. Therefore, this 2D material can provide enhanced mechanical interlocking at fibre-matrix interface, and fibre surface modification with GO appears a reasonable approach [15].

Various other techniques have been used and studied for carbon fibre surface modification, including plasma treatment, wet oxidation, electrochemical oxidation, γ-ray irradiation, ultrasonic treatment, chemical grafting and etching [16–21]. However, these are multistep procedures requiring complicated and costly instruments [22–24]. More importantly, these surface treatments are limited to strict reaction conditions and in some cases the use of toxic materials may damage fibre surface and ultimately reduce fibre strength [17,25–27].

A versatile and non-damaging route for modifying carbon fibre

---

* Corresponding author. Department of Materials, School of Natural Sciences, University of Manchester, Manchester, M13 9PL, United Kingdom.
E-mail addresses: xuqing.liu@manchester.ac.uk (X. Liu), xiaogang.chen@manchester.ac.uk (X. Chen).

https://doi.org/10.1016/j.compositesb.2021.108983
Received 28 March 2021; Received in revised form 17 April 2021; Accepted 9 May 2021

surface was developed in this work by using polydopamine (PDA) with the graphene oxide (GO) grafted on the fibre. PDA is a bio-inspired polymer, derived from the adhesive proteins in mussels [28–31]. It is shown that dopamine can self-polymerise and generate a PDA coating, which bonds to fibre surface and introduce functional groups under mild temperature, pH and time conditions [28,32–35]. This research examines and quantifies the effect of PDA coating and GO grafting on interfacial properties and tensile strength of a carbon fibre. The morphology and the chemical properties of the coatings were investigated, and the mechanical properties of the modified fibres were measured by the single fibre tensile test. The interfacial property between carbon fibre and epoxy resin was characterised by the microbond test.

2. Experimental details

2.1. Materials

The carbon fibres used in this research were type A-42 from AKSACA (USA) and treated by acetone to remove the manufacturer's sizing (a proprietary right), and the de-sized carbon fibres were marked as untreated fibre in this research. Dopamine hydrochloride, epoxy (AY103) and hardener (HY951) were purchased from Sigma-Aldrich® (UK), while the Tris(hydoxymethy)aminomethane (Tris) was acquired from Alfa Aesar Company (USA). Graphene oxide water dispersion (TM-01LI-06) was purchased from the Institute of Coal Chemistry, Chinese Academy of Sciences (China).

2.2. Fibre surface modification process

Dopamine solution was prepared by dissolving dopamine (2 mg/mL) in Tris-HCl buffer solution (1.2 mg/mL) and the pH was controlled at 8.5. The de-sized carbon fibre bundles were immersed in the self-oxidised dopamine solution. The surface treatment time were controlled for 1, 6, 12, 18 and 24 h, and the corresponding coated samples were coded as PDA 1 h to PDA 24 h, respectively.

For the GO-PDA treatment, the de-sized carbon fibre bundles were immersed into the dopamine solution and 0.1 mg/mL GO solution was added into the mixture. The treatment time were also controlled for 1, 6, 12, 18 and 24 h and the corresponding coated fibres were coded as GO-PDA 1 h to GO-PDA 24 h, respectively.

The specimens were then taken out of the solution, rinsed with distilled water three times, and dried in oven at 60 °C for 24 h. The schematic of carbon fibre preparation process is shown in Fig. 1. Two types of control specimens were prepared. GO-direct carbon fibre was prepared by immersing a bundle of carbon fibres into 0.1 mg/mL GO solution for 24 h, while the H_2SO_4 carbon fibre specimen was created by submerging the carbon fibre bundle in 98% sulfuric acid at ambient temperature for 24 h.

2.3. Preparation of carbon fibre/epoxy micro-droplet composites

One single carbon fibre was randomly chosen from the treated fibre bundle and set up to a rectangular frame. Then, a small droplet of epoxy resin and (AY103) and hardener (HY951) mixture was placed on the fibre using a needle point. The resin micro-droplet was cured at room temperature for 24 h.

2.4. Analysis and characterisation techniques

The morphology of carbon fibre surface was studied by a Scanning Electron Microscope (Ultra-55 SEM, ZEISS, Germany). The carbon fibre samples were sputter-coated with gold before observation.

The chemical structures of solution and fibre were investigated by Raman spectroscopy (Renishaw System 1000 Raman Spectrometer, Renishaw) with Modu-Laser 514 nm Argon-ion laser and the Fourier transform infrared spectroscopy (FTIR, Nicolet 5700, USA).

The chemical composition and functional groups on fibre were characterised by X-ray Photoelectron Spectroscopy (XPS, Kratos Axis Ultra Hybrid, Shimadzu, Japan) equipped with a monochromatic source of Al Kα, with base pressure below 5×10^{-8} mbar and spot area of 300 μm × 700 μm. The binding energy peaks were calibrated with C1s at 284.8 eV as reference.

The interfacial shear strength (IFSS) was measured by performing the microbond test. The IFSS between the single fibre and resin is given in Equation (1):

$$\mathrm{IFSS} = \frac{F}{\pi d_f L_e} \quad (1)$$

where F is the failure tensile load, d_f is the fibre diameter and $L_e$is the embedded length in the resin.

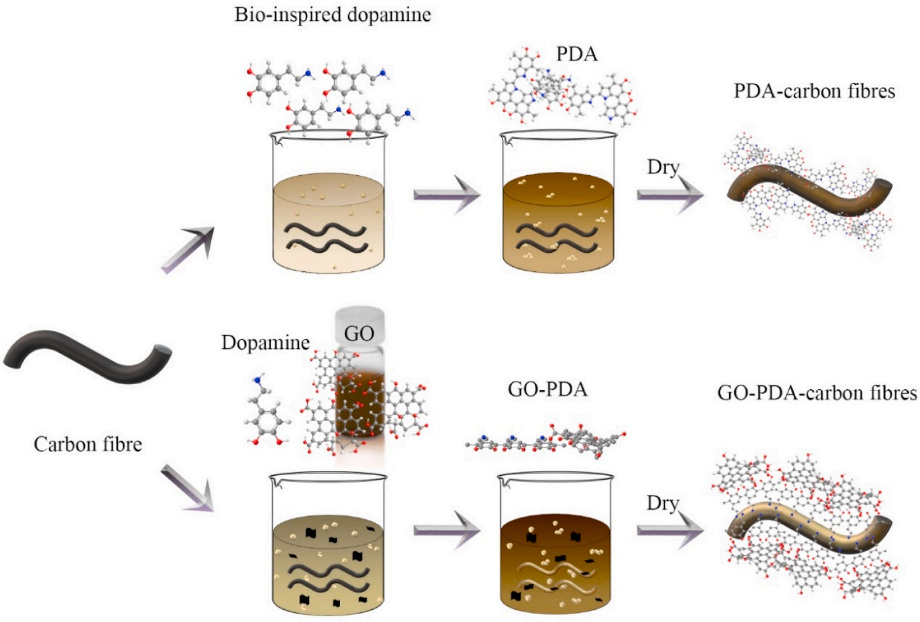

Fig. 1. Carbon fibre surface modification process with PDA treatment and GO-PDA treatment.

The single fibre tensile test was conducted on Instron 1122 with a 5 N load cell. According to ASTM D 3379-75 [36], the test was carried out at a constant speed of 1 mm/min. For each type of fibre examined, ten tensile tests were performed and the average strength and elastic modulus were obtained.

3. Results and discussion

3.1. Fibre surface characterisation

Fig. 2 displays the characterisation results of the fibre surfaces. The surface chemical structures of untreated, PDA treated and GO-PDA treated carbon fibre were detected by FTIR and Raman spectroscopy. The FTIR results were showed in Fig. 2 (a). The peaks appear at 3000-3500 cm^{-1} correspond to the asymmetric stretching vibrations of N-H and O-H bonds, while the ones at 2921 and 2852 cm^{-1} reflect the stretching vibrations of the C-H bonds. The peaks at 1620 cm^{-1} corresponded to C=C stretching vibration of indole. For the PDA-carbon fibre, the peaks at 1200, 1137 and 1060 cm^{-1} indicate the C-O bonds. There were no new peaks after PDA and GO-PDA treatment, only the intensity of the C-O group of PDA-carbon was higher than the C-O group intensity of untreated and GO-PDA-carbon. The FTIR results confirmed the successful coating of the carbon fibre surface. Compared to the untreated fibre, the chemical structure of the fibre under both PDA and GO-PDA treatment did not show any obvious change. The analysis confirmed that the PDA and GO-PDA treatment did not break the fibre bulk structure.

The Raman spectra of the fibre surfaces were shown in Fig. 2 (b). For the untreated carbon fibre, the Raman spectrum displayed two main characteristic peaks, which are important indicators of the structural defects in carbon-based materials. The D band at 1365 cm^{-1} corresponds to the conversion of sp^2-hybridized carbon to sp^3-hybridized carbon originated from the destruction of sp^2 structures of graphite or the covalent attachment of functional groups [37,38]. The D band is associated with amorphous carbon atoms, activated by some defects, such as edges, functional groups or structural disorders. The G band at 1591 cm^{-1} is intrinsic of graphite structure, corresponding to a well-defined sp^2-bonded carbon type. In the PDA treated carbon fibre Raman spectrum, there are three main characteristic peaks. The D band and G band are around 1381 cm^{-1} and 1575 cm^{-1}, respectively. The band around 2830 cm^{-1} is designated as the G′ band (or 2D), which was induced by a double-resonance effect and the overtone of the D band. The sharp G′ peak was always obtainable in almost defect-free samples [25,39]. Thus, as coated by a low ordered graphitic material, the PDA-carbon fibre showed a dispersive G′ band. Comparing PDA-carbon fibre with untreated carbon fibre, the shift of the D and G bands imply that the PDA coating fully covered surface of untreated carbon fibre. Also, the integral area ratio of D peak intensity to G peak intensity (I_D/I_G) was used to

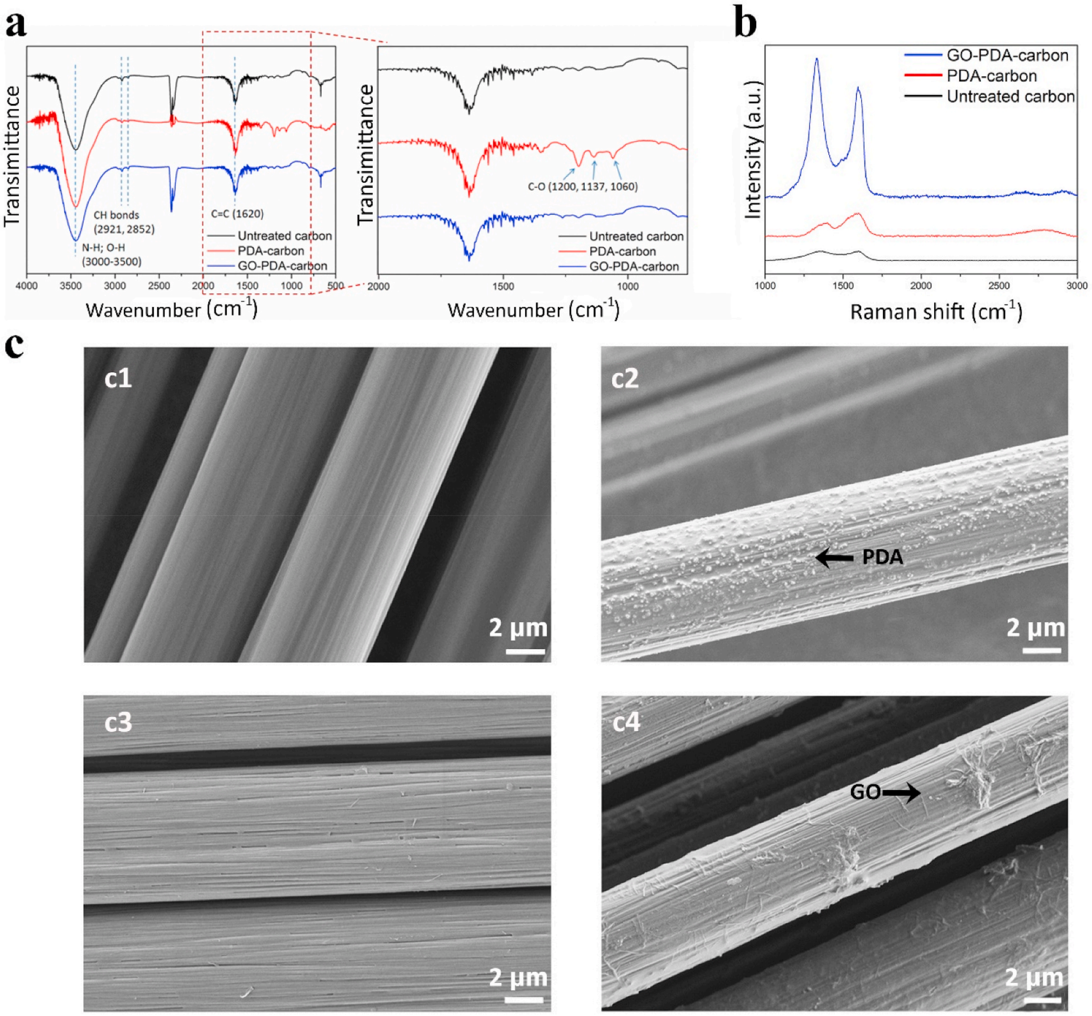

Fig. 2. Surface investigation on chemical compositions and morphology. (a) FTIR spectra of the untreated-, PDA 24 h- and GO-PDA 24 h-treated carbon fibre; the 750-2000 cm-1 spectra were enlarged. (b) Raman spectra of untreated, PDA treated and GO-PDA 24 h treated carbon fibre. (c) SEM micrographs of (c1) untreated, (c2) PDA 24 h treated, (c3) GO directly deposited on carbon fibre, and (c4) GO-PDA 24 h treated carbon fibres.

assess the degree of graphitisation, and it is understood that a higher I_D/I_G ratio indicates more defects and disorders of the graphitic materials [40,41]. The I_D/I_G ratio of untreated carbon fibre was 2.54, while for PDA-carbon fibre, the I_D/I_G ratio decreased to 0.55. The lower I_D/I_G ratio of PDA-carbon fibre suggested the formation of PDA molecules decreased the degree of disorder and the amorphous carbon atom number of carbon fibre surface. For the GO-PDA-carbon fibre, the D and G bands are around 1334 cm^{-1} and 1586 cm^{-1}, respectively. The Raman signal of PDA layer is weak compared to the signal of GO, and therefore the GO-PDA signal mainly showed the peaks of GO. The results showed that the I_D/I_G ratio of GO-PDA-carbon was 1.53, and that the G' band appeared at around 2830 cm^{-1}, both of which indicated the successful coating of PDA and GO-PDA on the carbon fibres.

The surface morphology of the various carbon fibres examined before and after the treatment was characterised by SEM. It can be seen in Fig. 2 (c1) that the untreated carbon fibres have microgrooves, and the surface is relatively smooth. After the PDA treatment, the SEM micrographs showed that the PDA layer fully covered the carbon fibre surface and the PDA-carbon fibres had an uneven surface with PDA agglomerates, which can increase the roughness of the fibre surface.

Fig. 2 (c3) shows the micrographs of carbon fibre directly immersed into 0.1 mg/mL GO solution. The GO-direct carbon fibre showed a clean surface with a small amount of GO flakes, which showed the inefficient and weak bonding between carbon fibre surface and GO without PDA. Fig. 2 (c4) shows the typical thin paper-like wrinkled GO morphology on GO-PDA 24 h carbon fibre surfaces, showing notable changes in the fibre surface morphology. With the GO-PDA 24 h treatment, the GO flakes were covered on carbon fibre surface, and some GO flakes were stacked together, which enhanced the roughness of the fibre surfaces. The SEM results further proved the successful coating of both PDA and GO-PDA layer on the carbon fibre surface.

For the PDA 24 h carbon fibre, after the dopamine self-polymerisation, the PDA tended to form a coating with the nano-sized agglomerates on the carbon fibre surface. However, for the GO-PDA 24 h carbon fibre, the increasing of the surface roughness mainly from the wrinkled structure of the GO. With the GO, the PDA tended to form a

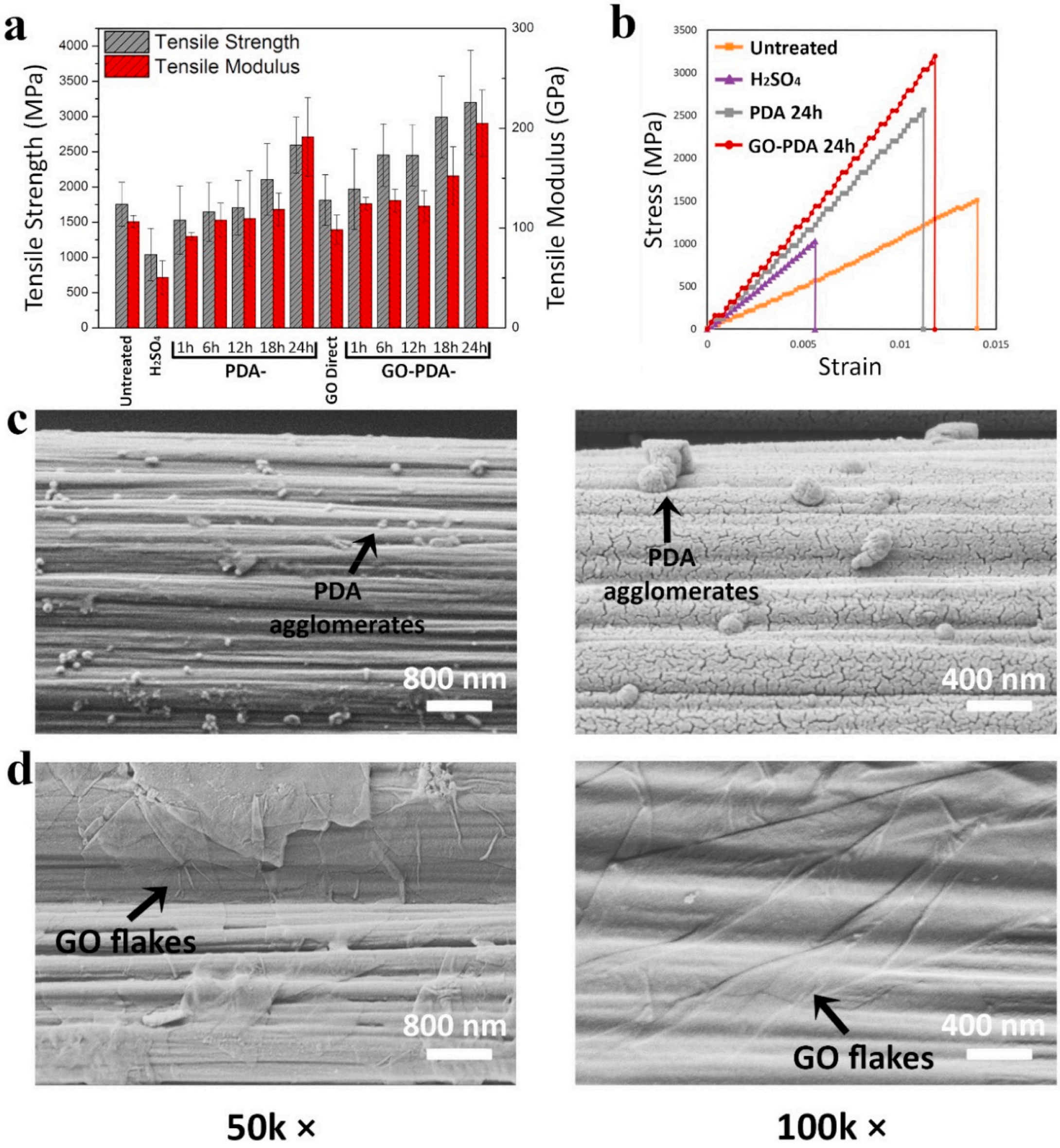

Fig. 3. The effect of the PDA and GO-PDA coating on fibre tensile properties: (a) Single fibre tensile strength and modulus of untreated, PDA- and GO-PDA treated carbon fibres. (b) Typical stress-strain curves for untreated, sulfuric acid treated, PDA- and GO-PDA treated single carbon fibres. SEM micrographs of (c) PDA 24 h carbon fibre and (d) GO-PDA 24 h carbon fibre at higher magnification (50 k and 100 k ×).

uniform 2D layer on the carbon fibre surface. This is because the PDA was templated by the 2D GO platelets, which formed micelles with certain nanoscale features in the liquid phase to guide the growth of the dopamine [42].

3.2. *Effect on the fibre tensile properties*

To investigate the effect of carbon fibre modification on tensile behaviour, single fibre tensile tests were conducted and the results are shown in Fig. 3 (a) and (b). For comparison, the fibre tensile strength and tensile modulus of untreated single carbon fibre were measured, giving 1756.7 ± 311.4 MPa and 106.4 ± 6.1 GPa, respectively. For the carbon fibre treated with sulfuric acid for 24 h, the tensile strength was reduced by 40.8% and the tensile modulus by 52.5%. After sulfuric acid treatment, carbon fibre surface was etched off. Although the sulfuric acid treatment could increase the fibre surface roughness, this method damaged the fibre structure and lowered its tensile strength and modulus. For both PDA and GO-PDA treated carbon fibre, the tensile strength and modulus increased with the increasing treatment time. The specimens that were treated by 24 h exhibited the highest average tensile strength and modulus. The tensile strength of PDA 24 h treated carbon fibre was increased to 2595.5 ± 396.4 MPa, representing a 47.8% increase comparing to the untreated carbon fibre, and the tensile modulus was increased by 79.9% to 191.4 ± 39.5 GPa. The large scatters in the tensile strength and modulus data are due to the high sensibility of the test and the variability of fibre bulk structures. Fig. 3 (c) shows SEM micrographs of PDA 24 h carbon fibre. It can be seen that the PDA layer fully coated the carbon fibre surface protecting the bulk structure. Also, the PDA agglomerates stacked on the fibre surface appear to have increased fibre surface roughness.

The single fibre tensile strength of GO-PDA treated-carbon fibre was increased to 3198.2 ± 741.7 MPa, which is 82.1% higher than that of the untreated de-sized carbon fibre. The tensile modulus of GO-PDA carbon fibre was increased by 92.7% over that of untreated de-sized carbon fibres. As shown in Fig. 3 (d), the GO-PDA layer covered the fibre surface and GO flakes stacked together to increase the roughness. These results revealed that the ultra-thin coating protected the fibre surface and filled the groves of the ordinary carbon fibre, which improved the tensile strength by reducing the stress concentration of the fibre. In addition, for the GO-PDA carbon fibres, the GO deposition on the fibre increased the surface roughness which provide extra resistance against the external loading [43]. The GO itself has superior mechanical properties, which also contribute the tensile strength improvement. Compared with sulfuric acid treatment, the PDA and GO-PDA treatment protected the bulk structure of carbon fibre and improved its tensile properties.

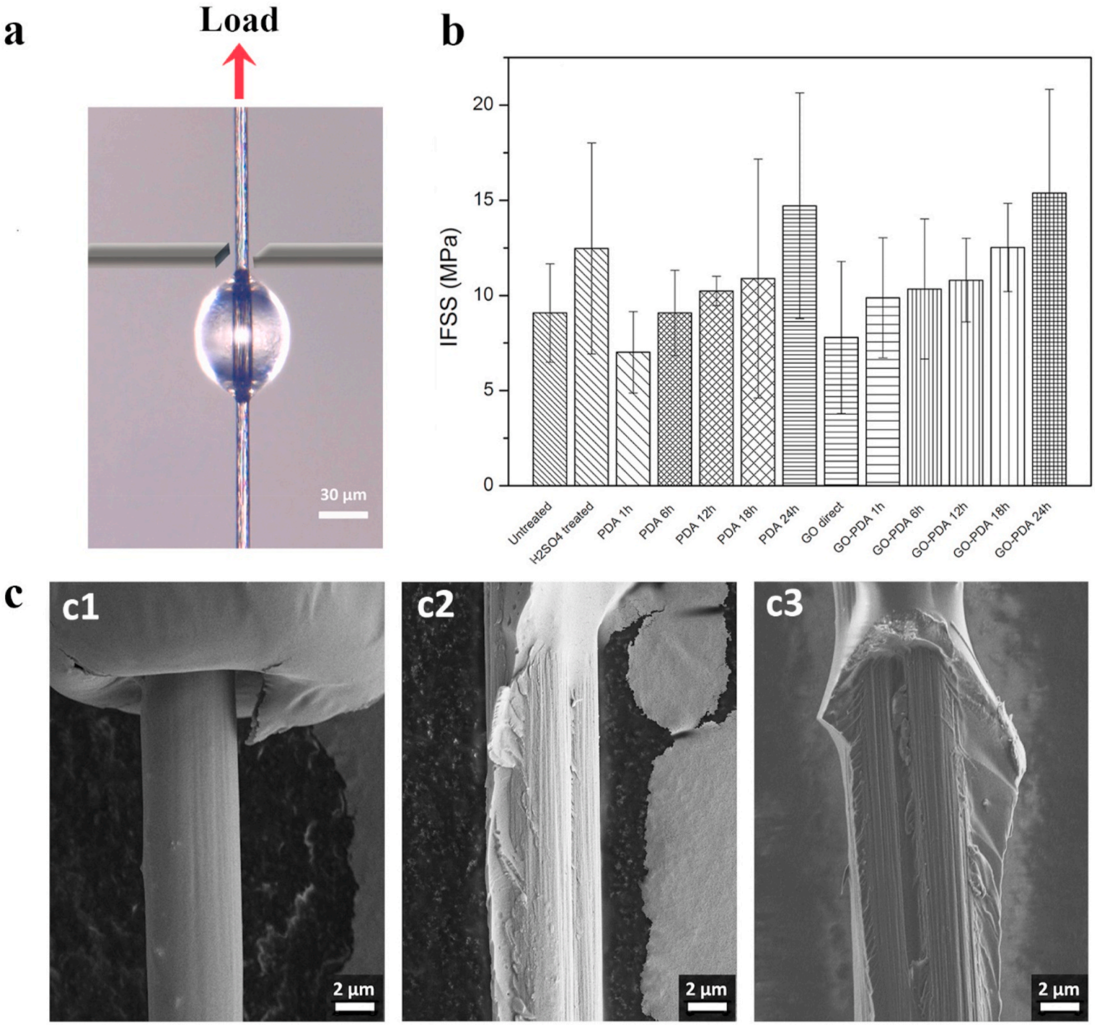

Fig. 4. The interfacial properties between fibre and epoxy resin: (a) The optical microscope image of microbond test specimen. (b) Interfacial shear strength between single carbon fibre and epoxy resin. (c) SEM micrographs of the fracture surface morphology after of (c1) untreated carbon fibre, (c2) PDA-carbon fibre and (c3) GO-PDA-carbon fibre/epoxy after microbond test.

3.3. *The fibre-resin interfacial properties*

The interfacial shear strength (IFSS) between carbon fibre and resin was investigated by pulling a fibre out of a resin droplet through a pair of knife-edges, and the microbond test specimen is shown in Fig. 4 (a). The IFSS results was shown in Fig. 4 (b). Compared with untreated carbon fibre, the IFSS of H_2SO_4 treated carbon fibre was increased 37.3%, since the treatment carved fibre surface and increase the fibre surface roughness. For both PDA and GO-PDA treated carbon fibre, the IFSS increased with the increasing treatment time. Compared with the untreated carbon single fibre/epoxy composites, the IFSS for the PDA 24 h carbon fibre composites increased from 9.1 MPa to 14.7 MPa, representing a 61.5% increase, and for the GO-PDA 24 h treated fibre composite, the IFSS was increased by 69.3% compared to the untreated one. The large scatter is due to the high sensitivity of the test, and each carbon fibre originally had different bulk structure due to the fibre manufacturing process. Each type of specimens was tested twenty times to obtain the average IFSS.

The IFSS increase can be attributed to the increased roughness of the fibre surface caused by PDA treatment and GO-PDA treatment. In addition, the successful grafting of GO introduced chemical groups which could also enhance the surface reactivity and polarity. Moreover, the addition of GO caused a random dispersion of particles within the regions surrounding carbon fibre, which offered a strengthening mechanism by bridging the surface microcracks [44]. The results revealed that the modification applied to the carbon fibre surface by polydopamine and graphene oxide effectively enhances the interfacial property of carbon fibre/epoxy composites.

The fracture surface morphology of single-fibre/epoxy composites after microbond test is shown in Fig. 4 (c). In micrbond test, the carbon fibre was pulled out of epoxy resin droplet. As shown in Fig. 4 (c1), the entire resin droplet slid away from the untreated carbon fibre surface with little residuals, indicating that the test broke the bonding between untreated carbon fibre and resin. In the case of pulling PDA treated carbon fibre, as shown in Fig. 4 (c2), some resin remained on the fibre surface after testing. The resin residuals imply that the load to break the bonding between PDA-carbon and resin was higher than the resin breaking load, which showed stronger bonding between PDA-carbon and resin than that between the untreated fibre and the resin. Fig. 4 (c3) shows more resin residuals on the GO-PDA treated fibres than that on the PDA treated one, further proving the improved bonding between the GO-PDA carbon fibre and the epoxy resin. The fact that the GO-PDA carbon fibre/matrix boundary was difficult to distinguish is an evidence of an effective bonding between the two phases. Such an enhanced interfacial adhesion would lead to a superior mechanical performance, which was in agreement with the microbond test results.

To investigate the chemical compositions and the bonding between PDA and GO-PDA coatings and the carbon fibre, the XPS was used to analyse the carbon fibre surfaces. The XPS C1s spectra were shown in Fig. 5. The fitting was done after a liner background subtraction on the fitting interval. The surface element compositions are listed in Table 1. Compared with the untreated carbon fibre, nitrogen was detected in PDA treated carbon fibre which proved the successful coating of PDA on carbon fibre surface. Meanwhile, PDA treated carbon fibre showed a higher O1s/C1s atomic ratio, due to the catechol and quinone groups of PDA polymer. This result is consistent with the FTIR results, confirming again the effective PDA coating. However, compared GO-PDA carbon fibre with PDA carbon fibre, the O1s/C1s decreased from 0.23 to 0.19. The intensity of O1s increased from untreated carbon fibre to PDA carbon fibre, and then decreased from PDA carbon fibre to GO-PDA

Table 1
Surface element compositions of untreated-, PDA- and GO-PDA-carbon fibre.

	Element composition [%]				
	C1s	O1s	N1s	O1s/C1s	N1s/C1s
Untreated carbon fibre	82.62	17.38	0	0.21	0
PDA carbon fibre	79.54	18.47	1.99	0.23	0.03
GO-PDA carbon fibre	83.24	15.49	1.27	0.19	0.02

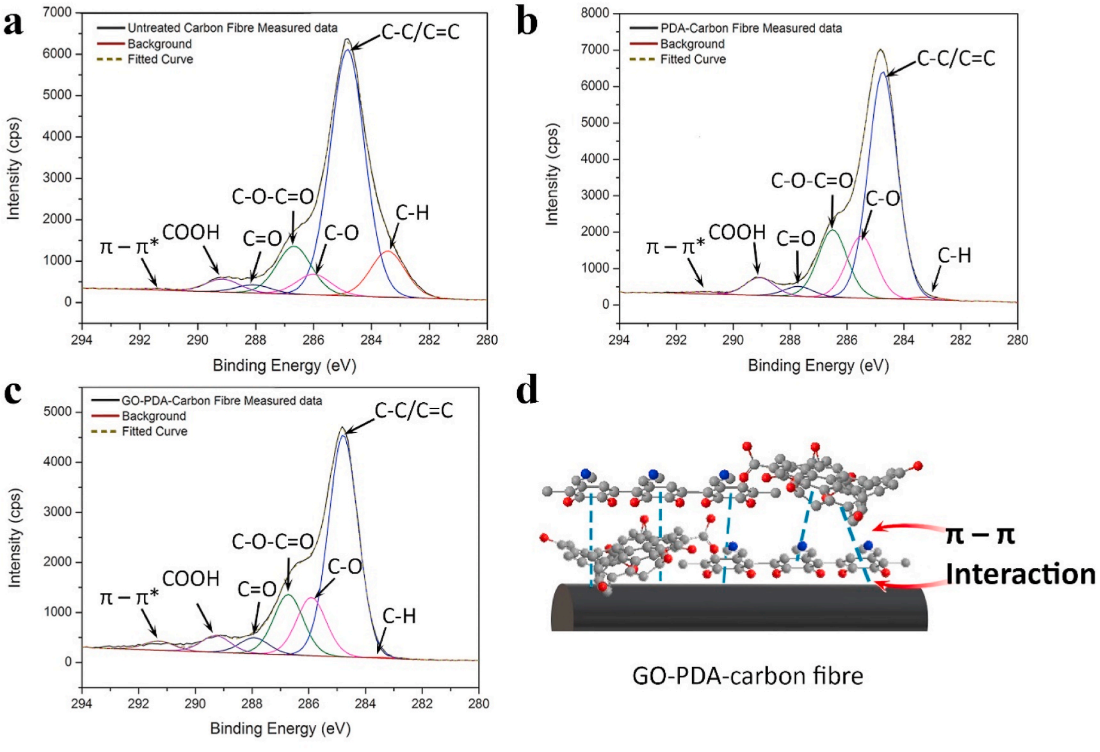

Fig. 5. The bonding between coatings and carbon fibre: High resolution XPS spectra of C1s of (a) untreated carbon fibre, (b) PDA-24 h carbon fibre, and (c) GO-PDA-24 h carbon fibre. (d) Schematic diagram of GO-PDA coating on carbon fibre surface by $\pi - \pi$ interaction.

carbon fibre, the intensity of N1s peaks also decreased from PDA carbon fibre to GO-PDA carbon fibre, which indicating that GO has been reduced to rGO.

For untreated carbon fibre, the C1s spectrum was peak fitted into seven fitting curves with peaks at 283.4, 284.8, 286.0, 286.7, 288.1, 289.1 and 291.5 eV, which are attributed to C-H, C-C/C=C, C-O, C-O-C=O, C=O, C(O)OH, and $\pi-\pi^*$, respectively [45,46]. The C1s spectrum of PDA treated carbon fibre was also fitted into seven curves (Fig. 5 (b)), and no new peaks emerged after PDA treatment. However, the ratio for oxygen-containing groups increased by 72.7% after PDA treatment, which mainly attributed to the fact that the intramolecular hydrogen bonding in carbon fibre was destructed which activates the originally inert fibre surface. The ratio of C-O groups of PDA-carbon was the highest, which were consistent with the FTIR results. The $\pi-\pi^*$ bonding increased from 0.36% to 0.62% by comparing the untreated carbon fibre with the PDA treated carbon fibre, which indicated the PDA was bonded with carbon fibres through $\pi-\pi$ interaction. The $\pi-\pi$ interaction is relating to the molecules' π-electron backbone system, to form a stable hybrid structure [47].

For GO-PDA treated carbon fibre, its XPS C1s core-level spectrum, shown in Fig. 5 (c) displays seven peak components with binding energies at about 283.4, 284.8, 285.9, 286.7, 288.0, 289.3 and 291.2 eV respectively, associating to the same function groups as the untreated carbon fibre. Compared to the untreated carbon fibre, the $\pi-\pi^*$ bonding of GO-PDA treated-carbon fibre significantly increased from 0.36% to 2.41%. The schematic diagram of the GO-PDA coating on the carbon fibre surface is shown in Fig. 5 (d). GO possessed sp2 structure and was homogenously distributed on carbon fibre. The extensive aromatic rings from the GO are essential for $\pi-\pi$ stacking interactions to take place. The GO was prone to attach on the fibre surface by $\pi-\pi$ interaction. The strong $\pi-\pi$ interaction between the GO surface and the aromatic molecules makes the surface stacking stable against rinsing or other solution processing [48,49]. It became evident that the GO-PDA treatment increased the surface activation of carbon fibre and thus increasing their interfacial adhesion strength.

4. Conclusions

This study provides a versatile method for surface modification of a chemically inert high-performance fibre, which dramatically improves interfacial shear strength that can be beneficial for intra- and inter-laminar crack resistance of modern fibre reinforced polymer composites. The bioinspired polydopamine and graphene oxide were used to improve the bonding between carbon fibre and epoxy resin. The results of SEM, Raman spectroscopy and FTIR confirmed that the carbon fibres were successfully coated by PDA and GO. The SEM micrographs displayed uniform coating of PDA and GO-PDA on the fibre surface, and they suggest that both PDA and GO-PDA treatments enhanced surface roughness of the fibre. XPS demonstrated that the $\pi-\pi^*$ bond was improved by coating PDA and GO-PDA. The strong $\pi-\pi$ interaction between the graphene oxide and the aromatic molecules usually makes the surface stacking stable, which improved interfacial shear strength between fibre and matrix. As a result, the interfacial shear strength of PDA 24 h treated carbon and GO-PDA 24 h treated carbon fibre composites were increased by 62% and 69%, respectively. In addition, both treatments protected the bulk structure of the carbon fibre. The PDA surface modification increased fibre tensile strength by 48%, while an 82% improvement was measured for the GO-PDA coated fibre. In conclusion, the polydopamine and graphene oxide surface treatments could result in enhanced interlaminar shear strength of laminated composite structures, preventing or delaying delaminations that can happen under relatively low energy impact events, something that could be considered in near future research. Such mechanical behaviour will be attractive to aerospace and other industries where high performance is required.

CRediT author statement

Lei Zeng: Investigation, Reviewing, Writing- Reviewing and Editing. **Xuqing Liu:** Conceptualisation, Methodology, Supervision. **Xiaogang Chen:** Conceptualisation, Methodology, Supervision. **Constantinos Soutis:** Conceptualisation, Methodology, Supervision. All authors read and contributed to the manuscript.

Declaration of competing interest

The authors declare that they have no known competing financial interests or personal relationships that could have appeared to influence the work reported in this paper.

Acknowledgement

The authors would like to thank the support of the Henry Royce Institute for Advanced Materials funded through EPSRC grants EP/R00661X/1, EP/P025021/1, and EP/P025498/1.

Appendix A. Supplementary data

Supplementary data to this article can be found online at https://doi.org/10.1016/j.compositesb.2021.108983.

References

[1] Simon R, Prosen S, Duffy J. Carbon fibre composites. Nature 1967;213(5081):1113.

[2] Schultz Ja, Lavielle L, Martin C. The role of the interface in carbon fibre-epoxy composites. J Adhes 1987;23(1):45–60.

[3] Keller T, Schollmayer M. Plate bending behavior of a pultruded GFRP bridge deck system. Compos Struct 2004;64(3–4):285–95.

[4] Hughes J. The carbon fibre/epoxy interface—a review. Compos Sci Technol 1991;41(1):13–45.

[5] McCarthy ED, Soutis C. Determination of interfacial shear strength in continuous fibre composites by multi-fibre fragmentation: a review. Composites Part A. Appl Sci Manuf 2019;118:281–92.

[6] Khandelwal S, Rhee KY. Recent advances in basalt-fiber-reinforced composites: tailoring the fiber-matrix interface. Compos B Eng 2020;192:108011.

[7] Mamalis D, Murray JJ, McClements J, Tsikritsis D, Koutsos V, McCarthy ED, et al. Novel carbon-fibre powder-epoxy composites: interface phenomena and interlaminar fracture behaviour. Compos B Eng 2019;174:107012.

[8] Terrones M, Martín O, González M, Pozuelo J, Serrano B, Cabanelas JC, et al. Interphases in graphene polymer-based nanocomposites: achievements and challenges. Adv Mater 2011;23(44):5302–10.

[9] Huang X, Qi X, Boey F, Zhang H. Graphene-based composites. Chem Soc Rev 2012;41(2):666–86.

[10] Rafiee MA, Rafiee J, Wang Z, Song H, Yu Z-Z, Koratkar N. Enhanced mechanical properties of nanocomposites at low graphene content. ACS Nano 2009;3(12):3884–90.

[11] Gnanasekar P, Chen H, Tratnik N, Feng M, Yan N. Enhancing performance of phosphorus containing vanillin-based epoxy resins by P–N non-covalently functionalised graphene oxide nanofillers. Compos B Eng 2021;207:108585.

[12] Lerf A, He H, Forster M, Klinowski J. Structure of graphite oxide revisited. J Phys Chem B 1998;102(23):4477–82.

[13] Szabó T, Berkesi O, Dékány I. DRIFT study of deuterium-exchanged graphite oxide. Carbon 2005;43(15):3186–9.

[14] Lerf A, He H, Riedl T, Forster M, Klinowski J. 13 C and 1 H MAS NMR studies of graphite oxide and its chemically modified derivatives. Solid State Ionics 1997;101:857–62.

[15] Hussain S, Yorucu C, Ahmed I, Hussain R, Chen B, Khan MB, et al. Surface modification of aramid fibres by graphene oxide nano-sheets for multiscale polymer composites. Surf Coating Technol 2014;258:458–66.

[16] Rong H, Dahmen K-H, Garmestani H, Yu M, Jacob KI. Comparison of chemical vapor deposition and chemical grafting for improving the mechanical properties of carbon fiber/epoxy composites with multi-wall carbon nanotubes. J Mater Sci 2013;48(14):4834–42.

[17] Sarmadi M. Advantages and disadvantages of plasma treatment of textile materials. In: 21st International Symposium on plasma Chemistry (ISPC 21); 2013. Sunday.

[18] Xing L, Liu L, Xie F, Huang Y. Mutual irradiation grafting on indigenous aramid fiber-3 in diethanolamine and epichlorohydrin and its effect on interfacially reinforced epoxy composite. Appl Surf Sci 2016;375:65–73.

[19] Li J, Cai C. The carbon fiber surface treatment and addition of PA6 on tensile properties of ABS composites. Curr Appl Phys 2011;11(1):50–4.

[20] Guo J, Lu C, An F, He S. Preparation and characterisation of carbon nanotubes/carbon fiber hybrid material by ultrasonically assisted electrophoretic deposition. Mater Lett 2012;66(1):382–4.

[21] Wang Y, Zhang S, Luo D, Shi X. Effect of chemically modified recycled carbon fiber composite on the mechanical properties of cementitious mortar. Compos B Eng 2019;173:106853.

[22] Ishifune M, Suzuki R, Mima Y, Uchida K, Yamashita N, Kashimura S. Novel electrochemical surface modification method of carbon fiber and its utilisation to the preparation of functional electrode. Electrochim Acta 2005;51(1):14–22.

[23] Li J-Q, Huang Y-D, Fu S-Y, Yang L-H. Qu H-t, Wu G-s. Study on the surface performance of carbon fibres irradiated by γ-ray under different irradiation dose. Appl Surf Sci 2010;256(7):2000–4.

[24] Zhang Y, Huang Y, Liu L, Cai K. Effects of γ-ray radiation grafting on aramid fibers and its composites. Appl Surf Sci 2008;254(10):3153–61.

[25] Vautard F, Ozcan S, Paulauskas F, Spruiell J, Meyer H, Lance MJ. Influence of the carbon fiber surface microstructure on the surface chemistry generated by a thermo-chemical surface treatment. Appl Surf Sci 2012;261:473–80.

[26] Boccaccini A, Schindler U, Krüger H-G. Ceramic coatings on carbon and metallic fibres by electrophoretic deposition. Mater Lett 2001;51(3):225–30.

[27] Käppler I, Hund R-D, Cherif C. Surface modification of carbon fibres using plasma technique. Autex Res J 2014;14(1):34–8.

[28] Lee H, Dellatore SM, Miller WM, Messersmith PB. Mussel-inspired surface chemistry for multifunctional coatings. Science 2007;318(5849):426–30.

[29] Sileika TS, Kim H-D, Maniak P, Messersmith PB. Antibacterial performance of polydopamine-modified polymer surfaces containing passive and active components. ACS Appl Mater Interfaces 2011;3(12):4602–10.

[30] Rodriguez-Emmenegger C, Preuss CM, Yameen B, Pop-Georgievski O, Bachmann M, Mueller JO, et al. Controlled cell adhesion on poly (dopamine) interfaces photopatterned with non-fouling brushes. Adv Mater 2013;25(42):6123–7.

[31] Wei Q, Haag R. Universal polymer coatings and their representative biomedical applications. Mater Horiz 2015;2(6):567–77.

[32] Yang H-C, Luo J, Lv Y, Shen P, Xu Z-K. Surface engineering of polymer membranes via mussel-inspired chemistry. J Membr Sci 2015;483:42–59.

[33] Liu Y, Ai K, Lu L. Polydopamine and its derivative materials: synthesis and promising applications in energy, environmental, and biomedical fields. Chem Rev 2014;114(9):5057–115.

[34] Zeng L, Liu X, Chen X, Soutis C. Surface modification of aramid fibres with graphene oxide for interface improvement in composites. Appl Compos Mater 2018;25(4):843–52.

[35] Yang W, Wu S, Yang W, Yuen AC-Y, Zhou Y, Yeoh G, et al. Nanoparticles of polydopamine for improving mechanical and flame-retardant properties of an epoxy resin. Compos B Eng 2020;186:107828.

[36] International A. ASTM D 3379-75Standard test method for tensile strength and Young's modulus for high-modulus single-Filament materials. 1989. p. 4.

[37] Dresselhaus MS, Dresselhaus G. Intercalation compounds of graphite. Adv Phys 2002;51(1):1–186.

[38] Bronikowski MJ, Willis PA, Colbert DT, Smith K, Smalley RE. Gas-phase production of carbon single-walled nanotubes from carbon monoxide via the HiPco process: a parametric study. Journal of Vacuum Science & Technology A. Vacuum, Surf Films 2001;19(4):1800–5.

[39] Yuan H, Wang C, Zhang S, Lin X. Effect of surface modification on carbon fiber and its reinforced phenolic matrix composite. Appl Surf Sci 2012;259:288–93.

[40] Vollebregt S, Ishihara R, Tichelaar F, Hou Y, Beenakker C. Influence of the growth temperature on the first and second-order Raman band ratios and widths of carbon nanotubes and fibers. Carbon 2012;50(10):3542–54.

[41] He L, Zhao P, Han Q, Wang X, Cai X, Shi Y, et al. Surface modification of poly-l-lactic acid fibrous scaffolds by a molecular-designed multi-walled carbon nanotube multilayer for enhancing cell interactions. Carbon 2013;56:224–34.

[42] Gao X, Mazloumi M, Cheung L, Tang XS. Graphene oxide film as a template for the creation of three-dimensional lamellar metal oxides and reduced graphene oxide/metal oxide hybrids. MRS Commun 2014;4(4):171.

[43] Wang C, Li J, Sun S, Li X, Zhao F, Jiang B, et al. Electrophoretic deposition of graphene oxide on continuous carbon fibers for reinforcement of both tensile and interfacial strength. Compos Sci Technol 2016;135:46–53.

[44] Zhang X, Fan X, Yan C, Li H, Zhu Y, Li X, et al. Interfacial microstructure and properties of carbon fiber composites modified with graphene oxide. ACS Appl Mater Interfaces 2012;4(3):1543–52.

[45] Jiang S, Li Q, Zhao Y, Wang J, Kang M. Effect of surface silanisation of carbon fiber on mechanical properties of carbon fiber reinforced polyurethane composites. Compos Sci Technol 2015;110:87–94.

[46] Nie W, Liu J, LIu W, Wang J, Tang T. Decomposition of waste carbon fiber reinforced epoxy resin composites in molten potassium hydroxide. Polym Degrad Stabil 2015;111:247–56.

[47] Zhang Z, Huang H, Yang X, Zang L. Tailoring electronic properties of graphene by π–π stacking with aromatic molecules. J Phys Chem Lett 2011;2(22):2897–905.

[48] Iqbal Z, Lai EP, Avis TJ. Antimicrobial effect of polydopamine coating on Escherichia coli. J Mater Chem 2012;22(40):21608–12.

[49] Henke P, Kozak H, Artemenko A, Kubát P, Forstová J. Mosinger Jí. Superhydrophilic polystyrene nanofiber materials generating O2 (1Δg): postprocessing surface modifications toward efficient antibacterial effect. ACS Appl Mater Interfaces 2014;6(15):13007–14.